ACADEMIA
ENVIRONMENTAL SCIENCES &
SUSTAINABILITY

Review Article
Published: 2025-04-04
https://doi.org/10.20935/AcadEnvSci7629

Rare earth recovery using metal–organic frameworks: advances, challenges, and future directions

Clint Sutherland[1,*]

Academic Editor: Martin Nuñez

Abstract

The field of study of rare earth element (REE) adsorption by metal–organic frameworks (MOFs) has emerged relatively recently. Recovering REEs from industrial, mining, and end-of-life electronics recycling effluents offers a sustainable approach to mitigating their unrestricted release into the environment. MOFs, known for their exceptional porosity and modifiability, have demonstrated significant potential as sustainable and efficient adsorbents for REE recovery from aqueous environments. To propel the advancement of this promising technology, a review of the fragmented research conducted over the past decade on REE adsorption by MOFs has been undertaken. Functionalization and combination of MOFs have proven effective in enhancing adsorbent capacity, stability, adsorption rate, and reusability. Notably, the 3D-agaric-like core–shell U6N@ZIF-8-20 MOF, MOF-bonded silica amine and polymer, and phosphonic acid–functionalized ZIF-67@SiO_2 MOF exhibited adsorption capacities of 341.0, 426.0, and 342.5 mg/g for Er^{3+}, Y^{3+}, and Ce^{3+}, respectively. Eluents such as HCl, HNO_3, and acetonitrile successfully achieved up to five adsorption–desorption cycles with minimal loss in adsorption efficiency. While MOFs are highly effective for REE adsorption, further advancements are needed in reducing equilibrium time, conducting fixed-bed column studies, and evaluating real-world wastewater to support their continued development.

Keywords: *adsorption, metal–organic frameworks, rare earth elements, adsorbent regeneration, adsorption mechanism*

Citation: Sutherland C. Rare earth recovery using metal–organic frameworks: advances, challenges, and future directions. *Academia Environmental Sciences and Sustainability* 2025;2. https://doi.org/10.20935/AcadEnvSci7629

1. Introduction

Rare earth elements (REEs) comprise a group of 17 metallic elements, including the 15 lanthanides from lanthanum (La) to lutetium (Lu) (**Figure 1**). Additionally, this group includes scandium (Sc) and yttrium (Y), which exhibit similar physicochemical characteristics [1]. According to Unsworth et al. [2], REEs can be categorized into light rare earth elements (LREEs) and heavy rare earth elements (HREEs), with HREEs being more economically valuable and less abundant.

Despite their name, REEs are relatively abundant in the Earth's upper continental crust, occurring in ion-adsorption clays and rare earth minerals in quantities comparable to common industrial metals such as nickel, chromium, copper, tin, and zinc [1]. However, Massari and Ruberti [3] highlighted a significant challenge with REEs: their uneven distribution in the environment. Identifying economically viable deposits is complex, and the similar chemical properties of these elements make their extraction and separation particularly challenging.

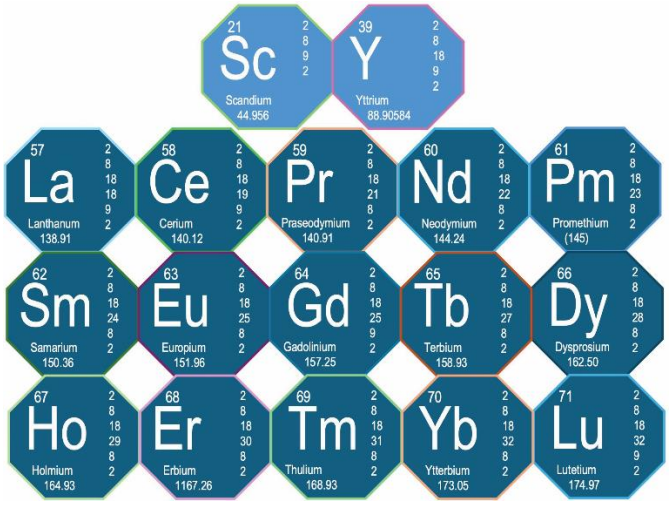

Figure 1 • Rare earth elements and their salient properties.

The global reserve of rare earth oxides is estimated at approximately 120 million tonnes, with major deposits found in China, Brazil, Russia, India, and Australia [4]. The production of REEs

[1]Project Management and Civil Infrastructure Systems, The University of Trinidad and Tobago, San Fernando, 602905, Trinidad and Tobago.
*email: clint.sutherland@utt.edu.tt

is highly resource-intensive, requiring energy of about 2,430 GJ/tonne REE and generating approximately 230 tonnes of CO_2-equivalent per tonne of total rare earth oxide [5, 6]. To put it into context, these energy demands and greenhouse gas emissions are an order of magnitude higher than those for steel production [7].

Due to their unique chemical, electrical, magnetic, and optical properties, REEs are utilized in various industries, including metallurgy, nuclear technology, and luminescence [8, 9]. As shown in **Figure 2**, they can also be combined with other elements or compounds to form products such as magnets, alloys, catalysts, and ceramics.

According to Wang et al. [10], REEs can enter the human body through dermal contact, inhalation, ingestion, and injections. These elements can cause dysfunctions in various organs and systems by affecting epigenetic, genetic, and signaling pathways. Numerous studies have highlighted health concerns associated with REE exposure. For instance, Cheng et al. [11] reported that lanthanide exposure in mice led to disturbed liver function and affected both cellular and humoral immunity. Liu et al. [12] found that exposure to lanthanides, such as La^{3+}, Gd^{3+}, and Yb^{3+}, caused changes in mitochondrial structure and membrane permeability in both animal and human cells. Brouziotis et al. [13] noted that REE mining can adversely affect human health, with these elements accumulating in the hair, urine, and blood of mining workers and people in nearby residents. In light of these findings, the authors cautioned that the eminent rise in REE demand could also present an exposure risk to e-waste recyclers and commuters in high-traffic environments. **Figure 3** illustrates the potential routes and dispersion of REEs in the environment.

Techniques such as precipitation and solvent extraction are well established for REE recovery, particularly in high-concentration and large-scale operations [14]. Van Nguyen et al. [15] explain that despite its widespread use, solvent extraction often involves co-extraction of other base metals, complicating the achievement of desired REE purity. Additionally, precipitation generates secondary waste and faces challenges in attaining low treatment levels. Other processes, such as electrocoagulation, show great potential, yet they are hindered by electrode consumption and secondary waste generation [16]. Membrane filtration can recover REEs with high efficiency, but it is energy-intensive, costly, and prone to membrane fouling [17]. In response to the growing global demand for REEs and the need to remediate REE-contaminated environments, significant research has focused on identifying and extracting REEs from new and recycled sources [5]. Recent studies have explored various sources, including e-waste [18], industrial waste [19], mine waste [20], fly ash [21, 22], phosphogypsum [23], red mud [24], mine tailings [25], acid mine drainage [26], and geothermal brines [5].

Figure 2 • Key applications of rare earth elements. MRI, magnetic resonance imaging.

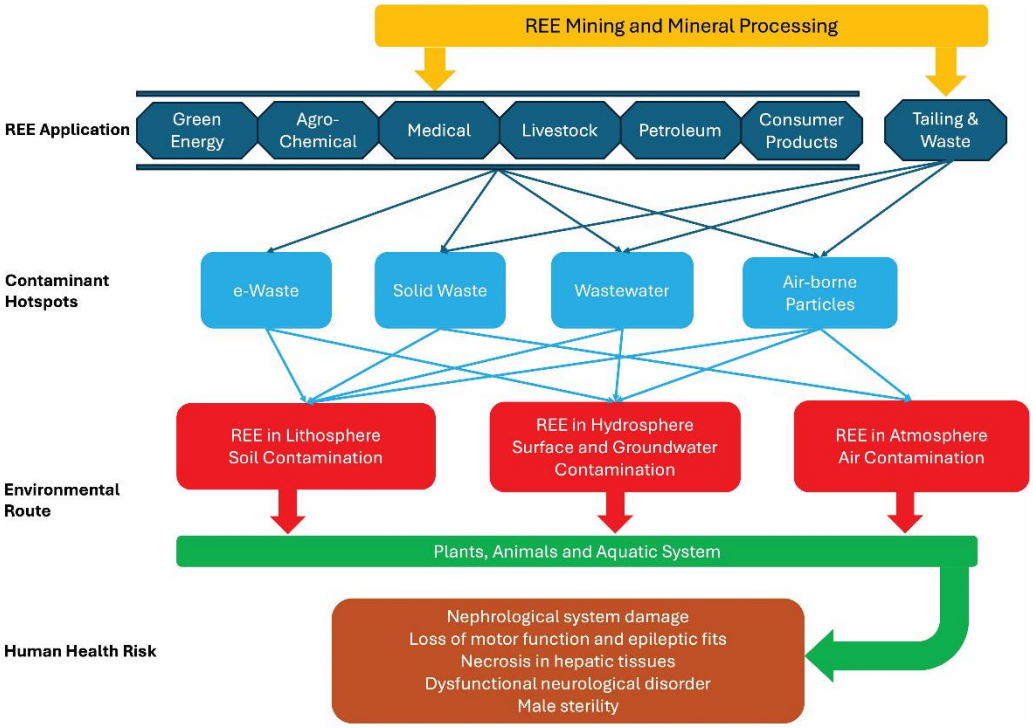

Figure 3 • Pathways for rare earth element contamination in the environment. REE, rare earth elements.

Adsorption technology offers numerous favorable characteristics, such as performance at low pH levels, adsorbent regeneration [14], low treatment levels, applicability to industries of various sizes, minimal secondary waste, high efficiency, ease of operation, and the ability to treat high volumes [27]. Various classes of adsorbents, based on their origin and characteristics, are currently being studied for their ability to remove and recover REEs from solutions. For instance, graphene oxide was used by Ashour et al. [28] for the adsorption of La^{3+}, Nd^{3+}, Gd^{3+}, and Y^{3+}, achieving adsorption capacities of 85.7, 188.6, 225.5, and 135.7 mg/g, respectively. Pinheiro et al. [29] reported promising performance in their report on the application of vine pruning waste-derived activated carbon for the adsorption of Ce^{3+} (48.5 mg/g) and La^{3+} (53.7 mg/g). Liu et al. [30] achieved the removal of 16.2 mg/g of Y^{3+} using montmorillonite clay. Gallardo et al. [31] investigated biosorption using natural, unmodified walnut shells and achieved maximum monolayer sorption capacities of 5.7, 6.0, 6.1, and 5.1 mg/g for Eu^{3+}, La^{3+}, Sm^{3+}, and Gd^{3+}, respectively. While adsorption offers numerous advantages, factors such as production cost, adsorbent reusability, and selectivity toward REEs in the presence of other metals can be uncertain and can vary depending on the adsorbent and treatment conditions [32, 33].

Metal–organic frameworks (MOFs) are classified as crystalline, porous organic–inorganic hybrid materials composed of metals or metal clusters (nodes) and multifunctional building blocks (linkers) [34]. These materials possess tunable pore sizes, ultrahigh surface areas, and adjustable internal surface properties [35].

To date, various synthesis methods have been successfully employed to develop MOFs, including hydrothermal [36], solvothermal [37], sonochemical [38], microwave-assisted [39], electrochemical [40], and mechanochemical [41]. Comprehensive insights into MOF synthesis and progressive development can be gleaned from studies conducted by Zhao et al. [42] and Huang et al. [43]. According to Essalmi et al. [44], the synthesis of MOFs as novel adsorbents can significantly reduce waste, minimize water usage, and involve fewer hazardous chemicals, presenting a potentially greener and more sustainable approach.

Since their first report by Yaghi et al. [45], MOFs have been successfully applied in various fields, including gas storage [46], drug delivery [47], catalysis [48], separation–adsorption [49], sensing [50], proton conduction [51], and biomedical imaging [52]. To date, MOFs have been widely studied for their applications in the adsorption of pesticides [53], antibiotics [54], and dyes [55]. They have also shown great promise in the adsorption of metal ions. For example, Bhadane et al. [56] recently developed a Cu-imidazolate MOF, which demonstrated exceptional reusability and performance for Pb^{2+} (492 mg/g), Cd^{2+} (327 mg/g), and Ni^{2+} (72.6 mg/g). Despite MOFs' remarkable physical adsorbent properties, their application in REE adsorption has been quite limited until recently. However, over the past decade, there have been great strides and recent momentum toward MOF improvements, adsorption optimization, and selectivity for REEs.

This narrative review focuses on examining the adsorption of REEs from aqueous solutions using MOFs. Studies published between 2014 and 2024 were sourced from international electronic databases, including Google Scholar, Scopus, PubMed, Web of Science, and ScienceDirect. The search employed keywords such as adsorption, rare earth elements, metal–organic framework, selectivity, and regeneration, using AND/OR operators in titles and abstracts.

Only original research articles were considered if they met the following criteria:

(1) the study involved laboratory research on REE adsorption from aqueous solutions using MOFs;

(2) the article was written in English;

(3) the publication date ranged from 2014 to 2024; and

(4) the full text was accessible.

Studies on MOF synthesis without adsorption experiments and those solely discussing theoretical adsorption mechanisms without experimental data were excluded. The reviewed studies showed that there are some gaps in the current research emphasis. In most instances, researchers focused on elucidating adsorption kinetics, equilibrium, characterization, selectivity, mechanisms, and MOF regeneration. However, little attention has been given to varying operational parameters, such as agitation, temperature, and adsorbent doses, which are essential for full-scale batch applications. Furthermore, as REE removal by MOF is a recent study area, most investigations are still at the laboratory batch scale, employing single contaminants in synthetic solutions.

Recently published reviews have focused on REE recovery using various technologies and various classes of adsorbents. This state-of-the-art review stands out as it specifically highlights the latest performance data on REE removal by MOFs and identifies key issues essential for process upscaling and development. To this end, the study consolidates scattered research and examines the preparation of MOFs, the influence of MOF properties, and the effects of operational parameters. Additionally, it assesses critical factors for process upscaling, such as the impact of solution pH on interactions and mechanisms between MOFs and REEs, adsorption modeling, MOF regeneration, and REE selectivity. The objective of this comparative approach is to highlight effective methods and current gaps, thereby facilitating the design of future studies.

2. Metal–organic framework preparation strategies and their application in rare earth element adsorption

Despite the advantageous attributes of MOFs, their structural stability in aqueous solutions and their affinity for REEs remain a challenge [32]. Huang et al. [43] explained that to address these issues, researchers have delved into the development of MOF-derived materials and MOF composites. Ligand modification in MOFs is a key strategy to enhance their properties for specific applications, including adsorption, catalysis, and gas storage [57]. These modifications can be broadly categorized into pre-synthetic (direct modification) and post-synthetic modifications. Recent research advances indicate that post-synthetic modification of MOFs with various functional groups has shown significant potential in improving REE selectivity and adsorption capacity.

De Decker et al. [58] emphasized that when designing a MOF, it must be able to withstand acidic environments, resist leaching, and avoid degradation during REE adsorption. Furthermore, incorporating functional groups that specifically target REEs—considering that lanthanides are hard Lewis acids—by using hard Lewis bases or combining synergistic moieties, such as amides and carbonyl groups, has been shown to enhance REE selectivity.

Another critical consideration in MOF selection for REE adsorption is the potential for metal exchange, where adsorbed metal ions may replace the MOF's own metal nodes or interact with pre-adsorbed metals within the framework. This exchange could compromise the structural stability of the MOF or lead to unintended metal contamination.

2.1. Metal–organic framework composites

De Decker et al. [58] functionalized chromium-based MIL-101 for the adsorption of Eu^{3+} from solution. The authors first synthesized MIL-101(Cr) using the hydrothermal method, followed by a three-step functionalization process. First, MIL-101(Cr) was chloromethylated. Next, a mixture of 1.0 g of the chloromethylated MOF, 2.2 g of 1,4-diaminobutane, and dimethylformamide (DMF) was stirred at 80°C for 24 h. Finally, the carboxylic end groups of diethylphosphonoacetic acid were coupled to the functionalized MOF using carbonyldiimidazole, producing a carbamoylmethylphosphine oxide (CMPO)–functionalized MIL-101(Cr).

The resulting adsorbent was successfully used to adsorb Eu^{3+}, achieving a maximum adsorption capacity of 12.5 mg/g at a pH of 4.0, a temperature of 25°C, and an equilibrium time of 5 h. The authors studied the effect of competing ions in synthetic solutions in the presence of Y^{3+} and Zn^{2+}, demonstrating the preferential uptake of Eu^{3+}. Such studies are particularly valuable for real-world applications, where REEs often coexist with other metal ions in industrial effluents. However, extending the selectivity analysis to actual wastewater samples would provide a more comprehensive understanding of its practical performance.

Another commendable aspect of the study is the stability assessment, which is often overlooked in similar research. The authors evaluated ligand leachability and the structural integrity of the adsorbent under acidic conditions, providing valuable data on its durability.

Liang and Zeng [59] also investigated MIL-101(Cr). Using MIL-101(Cr) as a base, they developed a unique adsorbent through post-synthetic modifications and radical polymerization to create MIL-101(Cr)-SMA-ED-PMG. Adsorption studies for Nd^{3+} and Eu^{3+} uptake demonstrated maximum sorption capacities of 102.7 and 110.4 mg/g, respectively, at a pH of 5.0 and an equilibrium time of 6 h.

A key strength of this study lies in its attempt to simulate real-world conditions. Unlike many laboratory-scale adsorption studies that rely solely on single-ion synthetic solutions, the authors tested Eu^{3+} removal from simulated zinc ore wastewater, achieving an impressive 92.2% recovery after three adsorption–desorption cycles. This highlights the reusability and robustness of MIL-101(Cr)-SMA-ED-PMG in complex matrices, a crucial factor for practical implementation.

2.2. Pristine metal–organic frameworks with defects

Zhang et al. [60] developed two MOFs with adjustable linker defects using benzoic acid as a modulator. These defective MOFs, designated as MIL-101(Cr)-D and MIL-101(Fe)-D, were employed for the adsorption of Yb^{3+} from solution. The adsorption mechanism was attributed to complexation. The sorbents MIL-101(Cr)-D and MIL-101(Fe)-D exhibited maximum sorption capacities of 27.9 mg/g and 37.5 mg/g, respectively, at a pH of 6.0 and a temperature of 30°C. Characterization studies revealed increased MOF porosity due to the introduction of defects and confirmed the coordination of Yb^{3+} with the oxygen sites of the Cr-O clusters.

Sun et al. [61] also developed defective MOFs, MOF-808-DLX and MOF-808-DSX, featuring abundant oxygen vacancies for the adsorption of Yb^{3+}. They reported adsorption capacities of 42.6 mg/g and 79.0 mg/g, respectively. Characterization studies

confirmed the mechanism to be complexation between the oxygen vacancies from Zr_6 clusters and the Yb^{3+} ions.

2.3. Pristine metal–organic framework

Zhou et al. [62] reported the development of an HKUST-1 MOF for the adsorption of Ce^{3+} from solution. The authors used a modified solvothermal technique to synthesize the adsorbent. A mixture of trimesic acid, copper(II) nitrate trihydrate, and N,N-dimethylformamide (DMF) was prepared and transferred to a Teflon-lined autoclave, which was heated at 75°C for 24 h. The specimen was then washed with DMF and dried in a vacuum oven at 150°C for 12 h. The resulting adsorbent had a Brunauer–Emmett–Teller (BET) specific surface area of 1,187 m^2/g, a total pore volume of 0.61 cm^3/g, and a mean pore diameter of 2.1 nm. A maximum adsorption capacity of 353.0 mg/g was achieved at a pH of 6.0 and an equilibrium time of 8 h. The isothermal and kinetic data were best represented by the Langmuir and pseudo-second-order equations, respectively. The authors suggested that Ce^{3+} elution with HCl indicated the influence of electrostatic interactions, while Raman spectroscopy revealed a secondary adsorption mechanism involving covalent bonding activity. Despite these strengths, the study had a few limitations. Experiments were conducted only in synthetic solutions, omitting the competitive ion effects common in real wastewater. While desorption tests were performed, the long-term stability and reusability of HKUST-1 remain unassessed. Future research should, therefore, evaluate selectivity in complex matrices, optimize regeneration strategies, and assess long-term stability.

Ammari Allahyari et al. [63] reported the development of a synthesized MOF, $[Zn(bim)_2(bdc)]_n$, for the adsorption of La^{3+} from solution. The authors synthesized the adsorbent by mixing 1,4-benzenedicarboxylic acid (H_2bdc), benzimidazole (bim), zinc acetate ($Zn(OAc)_2{\bullet}3H_2O$), sodium hydroxide, and distilled water. This mixture was agitated in an autoclave at 140°C for 72 h. Subsequently, the mixture was left to cool at room temperature for seven days. Batch adsorption studies indicated that the isothermal and kinetic data were best represented by the Langmuir and pseudo-first-order equations, respectively. Thermodynamic analysis showed that the process was feasible, spontaneous, and endothermic in nature, highlighting the strong influence of covalent bonding due to the high enthalpy. The maximum monolayer capacity was found to be 135.0 mg/g at a pH of 7.0 and an equilibrium time of 2.5 h. The rate-limiting step was evinced using the shrinking core model, which concluded that interfacial resistance was the major mechanism.

A notable strength of this study is its laboratory-scale column adsorption experiments, a fundamental step toward real-world application. The authors conducted laboratory-scale column adsorption studies with a column diameter of 0.8 cm, a height of 30 cm, an adsorbent mass of 0.05 g, an initial concentration of 25 mg/l, and a flow rate of 0.26 ml/min. The dynamic capacity (156.7 mg/g) exceeded batch adsorption results by 20%, demonstrating enhanced performance under continuous flow. However, the study lacked competitive ion assessments, which are essential for evaluating selectivity in complex matrices. Future research should focus on assessing adsorbent regeneration and testing the performance of $[Zn(bim)_2(bdc)]_n$ in real wastewater systems.

3. Comparison of metal–organic frameworks with conventional adsorbents for rare earth element adsorption

Over the past decade, the application of MOFs for REE adsorption has steadily increased. **Table 1** presents key features of these studies, showing that MOFs compare favorably with conventional adsorbents in the literature. For example, Komnitsas et al. [64] utilized commercial activated carbon to adsorb Sc^{3+} and Nd^{3+}, achieving maximum sorption capacities of 8.8 and 8.5 mg/g, respectively. By contrast, Liang and Zeng [59] and Zhang et al. [65] reported significantly higher capacities for Nd^{3+} using MOF adsorbents MIL-101(Cr)-SMA-ED-PMG (102.7 mg/g) and U6N@ZIF-8-20 (249.9 mg/g), respectively. Similarly, Lou et al. [66] achieved a Sc^{3+} sorption capacity of 90.2 mg/g using the 0.075-AA-0.072@MIL-101 MOF. Comparatively, these MOF adsorbents evinced at least a tenfold increase in capacity over the referenced commercial activated carbon.

Table 1 • Selection of metal–organic framework performances for the uptake of rare earth elements from synthetic solutions

Adsorbent	Adsorbent abbreviation	Adsorbate	pH	Time (min)	Adsorption capacity (mg/g)	Ref.
Functionalized chromium-based MIL-101 MOF	CMPO@MIL-101(Cr)	Eu^{3+}	4.0	300	12.5	[58]
Copolymer-functionalized MIL-101(Cr)-SMA-ED-PMG MOF	MIL-101(Cr)-SMA-ED-PMG	Eu^{3+}	5.0	360	110.4	[59]
3D-agaric-like core–shell U6N@ZIF-8-20 MOF	U6N@ZIF-8-20	Eu^{3+}	5.0	10	295.3	[65]
Organophosphorus-modified MIL-101(Cr) MOF	MIL-101-H50	Er^{3+}	5.5	1,440	57.5	[32]
3D-agaric-like core–shell U6N@ ZIF-8-20 MOF	U6N@ZIF-8-20	Er^{3+}	5.0	10	341.0	[65]
Post-synthetic MIL-101(Cr)-SMA-ED-PMG MOF	MIL-101(Cr)-SMA-ED-PMG	Nd^{3+}	5.0	360	102.7	[59]
3D-agaric-like core–shell U6N@ZIF-8-20 MOF	U6N@ZIF-8-20	Nd^{3+}	5.0	10	249.9	[65]

Linker-defective MIL-101(Cr)-D MOF	MIL-101(Cr)-D	Yb^{3+}	6.0	-	27.9	[60]
Linker-defective MIL-101(Fe)-D MOF	MIL-101(Fe)-D	Yb^{3+}	6.0	-	37.5	[60]
Linker-defective MOF-808-DLX MOF	MOF-808-DLX	Yb^{3+}	-	-	42.6	[61]
Linker-defective MOF-808-DSX MOF	MOF-808-DSX	Yb^{3+}	-	-	79.0	[61]
HKUST-1 MOF	HKUST-1 MOF	Ce^{3+}	6.0	480	353.0	[62]
Phosphonic acid–functionalized ZIF-67@SiO_2	P-MNPC@SiO_2	Ce^{3+}		20	342.5	[67]
Synthesized MOF $[Zn(bim)_2(bdc)]_n$	$[Zn(bim)_2(bdc)]_n$	La^{3+}	7.0	150	135.0	[63]
Phosphonomethyl iminodiacetic acid–functionalized MOF	PMIDA@FeBTC	La^{3+}	6.0	-	232.5	[68]
Acrylic acid–functionalized MOF 0.075-AA-0.072@MIL-101	0.075-AA-0.072@ MIL-101	Sc^{3+}	4.5	300	90.2	[66]
MOF-bonded silica amine and polymer	ZnGA–Si–NH–PC	Y^{3+}	7.0	30	426.0	[69]
3D-agaric-like core–shell U6N@ ZIF-8-20 MOF	U6N@ZIF-8-20	Gd^{3+}	5.0	10	316.2	[65]
Functionalized MOF MIL-101-PMIDA	MIL-101-PMIDA	Gd^{3+}	5.5	360	90.0	[70]
Lanthanum-based MOF LaBDC@50%PEI	LaBDC@50%PEI	Gd^{3+}	5.5	180	181.8	[71]
Zinc-trimesic acid (Zn-BTC) MOF/nanoporous graphene	Zn-BTC MOF/NG	Pr^{3+}, Sm^{3+}, Tb^{3+}, Dy^{3+}, Ho^{3+}, Tm^{3+}, and Lu^{3+}	2.0	160	29.6, 30.4, 12.2, 9.9, 7.4, 5.5, and 5.3	[72]

MOF, metal–organic framework.

Additionally, Iannicelli-Zubiani et al. [73] reported an adsorption capacity of 94.5 mg/g for La^{3+} using commercial activated carbon at pH 6.0 with an equilibrium time of 30 min, whereas Ammari Allahyari et al. [63] achieved a comparable 135.0 mg/g using the MOF $[Zn(bim)_2(bdc)]_n$ at pH 7.0 but with a longer equilibrium time of 150 min. Hamed et al. [74] investigated Gd^{3+} adsorption on Dowex HCR-S/S cation exchange resin, reporting a monolayer adsorption capacity of 66.0 mg/g within a pH range of 2.0–7.0 and an equilibrium time of 40 min. Meanwhile, Lee et al. [70], Li et al. [71], and Zhang et al. [65] reported significantly higher adsorption capacities of 90.0, 181.8, and 316.2 mg/g for MIL-101-PMIDA, LaBDC@50%PEI, and U6N@ZIF-8-20, respectively.

Remarkably, Zhang et al. [65] demonstrated that by combining UiO-66-NH_2 and ZIF-8 MOFs to create U6N@ZIF-8-20, exceptional performance was achieved within just 10 min of contact. This synergy is particularly significant given the inherent stability and robustness of zeolitic imidazolate frameworks (ZIFs) [57]. Among them, ZIF-8 has been extensively studied for its remarkable resistance to both acidic and basic environments, making it a highly promising sorbent for REE removal from wastewater. Likewise, UiO-66 is one of the most chemically stable MOFs [75], possessing strong Zr–O coordination bonds and high thermal resistance, which enhance its durability and reusability in adsorption applications.

Overall, MOFs have exhibited excellent performance in REE adsorption compared to conventional adsorbents. To advance toward full-scale applications, future research needs to focus on real wastewaters containing multiple competing and coexisting ions, a broader range of REEs, and moving beyond synthetic single-contaminant scenarios.

4. The impact of contact time on metal–organic framework adsorption of rare earth element

The contact duration between the adsorbate and the adsorbent does not directly affect adsorption capacity; however, it can be a limiting factor, as prolonged contact allows the adsorbent to achieve its maximum capacity [76]. Therefore, optimizing contact time is crucial, as it directly impacts operational costs and thereby influences the feasibility of using the adsorbent in full-scale applications. The performance of MOFs in relation to contact time is detailed in **Table 1**. Notably, Mahmoud et al. [69], Xu et al. [67], and Zhang et al. [65] stand out with equilibrium times of 30, 20, and 10 min, respectively. In each case, kinetic curves showed rapid initial uptake, followed by a gradual approach to equilibrium. While authors attributed this gradual approach to varying theories, most postulated that the rapid uptake resulted from the abundance of vacant sites during the initial adsorption stages, with adsorption slowing as sites became occupied.

Zhang et al. [65] achieved equilibrium within 10 min of U6N@ZIF-8-20 contact with Nd^{3+} ions in solution. The authors attributed this profound performance to the concentration gradient created by the high initial concentration and the abundant, highly accessible active sites of U6N@ZIF-8-20. Similarly, Lou et al. [66] observed that 63% of Sc^{3+} adsorption capacity by 0.075-AA-0.072@MIL-101 was attained within the first 5 min, with equilibrium reached after 5 h. The authors explained that the rapid uptake was due to the large number of carboxyl functional groups on the adsorbent surface. Based on kinetic data analysis, they further concluded that the slow approach to equilibrium was limited by chemical sorption. However, Lee et al. [70] attributed the slow equilibrium attainment of MIL-101-PMIDA to the slow diffusion of Gd^{3+} ions into the adsorbent matrix.

From the reviewed studies presented in **Table 1**, the average time to reach equilibrium was approximately 4.5 h, which does not compare favorably with conventional adsorbents. Therefore, future research should prioritize on reducing equilibrium times to enhance competitiveness with established adsorbents.

5. Metal–organic framework selectivity of rare earth element

In real-world scenarios, an adsorbent's preferential selectivity for specific REE species is crucial. In practical applications, wastewaters typically contain a mix of multivalent ions that compete for available adsorption sites on the adsorbent surface, potentially impacting REE uptake. Assessing selectivity in adsorption systems involves evaluating an adsorbent's preference for one particular adsorbate over others in a mixture.

Table 2 presents the criteria used to assess selectivity, which varied among researchers. Lee et al. [70] studied Gd^{3+} adsorption by MIL-101-PMIDA, reporting a selectivity of 90% for Gd^{3+} over other transition ions. Among the transition ions studied, trivalent cations Al^{3+} and Fe^{3+} were preferentially adsorbed compared to lower-valency ions, such as Co^{2+}, Ni^{2+}, and Zn^{2+}. Li et al. [71] also demonstrated that LaBDC@50%PEI had a strong affinity for Gd^{3+} even in the presence of Na^+, NH_4^+, Ca^{2+}, Mg^{2+}, and Al^{3+}. Mono- and divalent cations had negligible effects on Gd^{3+} adsorption, while the presence of trivalent ions like Al^{3+} allowed LaBDC@50%PEI to still retain 83% of its original adsorption capacity for Gd^{3+}.

Luo et al. [66] compared the selectivity of Sc^{3+} against 16 other REEs on a one-on-one basis and found that above pH 2.0, the adsorbent 0.075-AA-0.072@MIL-101 exhibited greater selectivity for Sc^{3+} over all other REEs. The authors assessed the selectivity by calculating a selectivity coefficient, as shown in **Table 2**, which exceeded 1.5 at pH ≥ 2.0. This high affinity was attributed to the small radius of Sc^{3+} and its strong interaction with the –OH and C = O groups of carboxyl on the adsorbent.

The selectivity of Eu^{3+} in the presence of Y^{3+} and Zn^{2+} was reported by De Decker et al. [58] and assessed using a distribution coefficient (K_d) and a separation factor (SF) as metrics (**Table 2**). The K_d values for Eu^{3+}, Y^{3+}, and Zn^{2+} were 149, 48, and 17, respectively. The SF revealed that the adsorbent exhibited a preference for Eu^{3+} over Y^{3+} with a factor of 3.2 and an even higher preference for Eu^{3+} over Zn^{2+} with a factor of 8.5.

Kavun et al. [32] studied the selectivity of Er^{3+} over transition ions (Cu^{2+}, Co^{2+}, Ni^{2+}, and Zn^{2+}) and light REEs (Nd^{3+} and Gd^{3+}) using the adsorbent MIL-101-H50. In the presence of transition ions, MIL-101-H50 demonstrated over 90% selectivity for Er^{3+}. A selectivity coefficient was calculated, as shown in **Table 2**, and revealed strong REE affinities with coefficients of 22.8 and 7.7 for Er^{3+}/Nd^{3+} and Er^{3+}/Gd^{3+}, respectively. These authors justified MOF functionalization based on the applicability of the hard and soft acid and bases (HSAB) theory in MOF adsorption of REEs. They demonstrated that hard base groups on adsorbents, such as carboxyl, phosphonic, and carbonyl groups, exhibit high selectivity toward hard acids like REE^{3+} ions. Additionally, the presence of $–NH_2$ groups on the adsorbent was reported to synergize with these other groups, further enhancing the attraction of REE ions.

Table 2 • Selectivity of rare earth elements by various metal–organic frameworks

Adsorbent	Adsorbate	Selectivity criteria	Initial conc. (mg/L)	pH	Competing ions/ (selectivity)	Ref.
MIL-101-PMIDA	Gd^{3+}	$\text{Sel }\% = \frac{\left(q_{e,\text{Target}}\right)*100}{q_{e,\text{Total}}}$	50	5.5	Co^{2+}, Ni^{2+}, Zn^{2+}, Al^{3+}, Fe^{3+}/(10%)	[70]
LaBDC@50%PEI	Gd^{3+}	$\text{Sel }\% = \frac{\left(q_{e,\text{Target}}\right)*100}{q_{e,\text{Total}}}$	100	5.5	Na^+, NH_4^+, Ca^{2+}, Mg^{2+}, Al^{3+}/(17%)	[71]
CMPO@MIL-101(Cr)	Eu^{3+}	$K_d = \frac{\left(C_o - C_e\right)}{C_e}\frac{V}{m}$; $\text{SF}_{a/b} = \frac{K_{d,a}}{K_{d,b}}$	50	5.0	Y^{3+}/(SF = 3.2) Zn^{2+}/(SF = 8.5)	[58]
0.075-AA-0.072@MIL-101	Sc^{3+}	$\text{Sel}_{a/b} = \log\left[\frac{\frac{q_{e,a}}{C_{e,a}}}{\frac{q_{e,b}}{C_{e,b}}}\right]$	20	1-4	All REE/(Sel = 1.5 for pH ≥ 2.0)	[66]
MIL-101-H50	Er^{3+}	$\text{Sel }\% = \frac{\left(q_{e,\text{Target}}\right)*100}{q_{e,\text{Total}}}$	50	5.5	Cu^{2+}, Co^{2+}, Ni^{2+}, Zn^{2+}/(<10%)	[32]
MIL-101-H50	Er^{3+}	$S_{a/b} = \frac{q_{e,a}}{q_{e,b}}$	100	5.5	Nd^{3+}/(S = 22.8), Gd^{3+}/(S = 7.7)	[32]

6. Mechanisms of metal–organic framework adsorption of rare earth elements

This section discusses the various approaches researchers have used to elucidate adsorption mechanisms, including thermodynamics, kinetics and equilibrium modeling, characterization studies, and pH variations. Thermodynamic analysis is a valuable tool in adsorption studies, offering insights into the feasibility, efficiency, mechanism, and optimization of adsorption processes. However, only a limited number (25%) of the reviewed studies have delved into thermodynamic analysis. For instance, Lou et al. [66] examined the impact of temperature on the adsorption of Sc^{3+} by 0.075-AA-0.072@MIL-101, concluding that the process is spontaneous and exothermic. Similarly, Zhang et al. [65] found the adsorption of Nd^{3+} by U6N@ZIF-8-20 to be spontaneous, with the degree of spontaneity increasing with temperature, indicating a chemical rather than physical process. Ammari Allahyari et al. [63] reported comparable findings for La^{3+} adsorption by $[Zn(bim)_2(bdc)]_n$, noting that positive entropy values suggest the reaction's irreversibility. It is noteworthy that Saha and Chowdhury [77] emphasized that while adsorption kinetics and isotherms have a robust theoretical foundation, the thermodynamic analysis of adsorption processes lacks comprehensive theoretical underpinnings. Therefore, thermodynamic analysis can serve as a useful guide for researchers; however, it is insufficient on its own for drawing definitive mechanistic conclusions.

Solution pH is another fundamental parameter in the adsorption process design, as it influences both the adsorbent's surface charge and the ionization of the adsorbate [78]. Lee et al. [70] found that the point of zero charge (pH_{pzc}) for MIL-101-PMIDA occurs at pH 3.0. Below this pH, the surface becomes positively charged, repelling Gd^{3+} ions. Above pH 3.0, the adsorption capacity increases up to pH 5.5 (**Table 1**). The deprotonation of adsorption sites on the adsorbent surface was responsible for the high performance at pH 5.5. Li et al. [71] also studied Gd^{3+} adsorption, maintaining a pH between 1.5 and 6.5. They reported maximum adsorption at pH 5.5, attributing this to the negatively charged functional groups on the adsorbent, which increased electrostatic attraction and complexation mechanisms. Similarly, Zhao et al. [62] demonstrated that pH profoundly affects the stability and adsorption capacity of HKUST-1. Between pH 2 and 4, HKUST-1 experienced increased decomposition, whereas at pH 6.0, its optimal pH for Ce^{3+} adsorption remained highly stable, partly due to electrostatic attraction. In all reviewed instances, the authors maintained the solution pH below 7.0 to prevent REE precipitation. The optimal pH for REE adsorption by MOFs was generally observed in slightly acidic conditions. This favorable pH range suggests that MOF technology could potentially reduce the costs associated with wastewater pH conditioning, enhancing its practical applicability.

To further elucidate the mechanisms of MIL-101-PMIDA adsorption of Gd^{3+}, Lee et al. [70] examined the FTIR spectra of the adsorbent before and after Gd^{3+} adsorption. The authors confirmed the participation of amine, phosphonic, and carboxyl functional groups. Based on zeta-potential analysis, Fourier transform infrared spectroscopy (FTIR), and pH analysis, they concluded that at a pH of 5.5, the mechanism was controlled by the complexation of deprotonated functional groups and electrostatic attraction between Gd^{3+} and $-NH_2OH^-$. A detailed examination of the reviewed literature revealed that MOF/REE isothermal and kinetic data were best represented by the pseudo-second-order and Langmuir equations. Both equations were developed on the premise that the reaction is limited by chemisorption [76, 79]. Lou et al. [66] analyzed equilibrium and kinetic modeling, which alluded to chemical interactions, then followed up with FTIR, X-ray photoelectron spectroscopy (XPS), and pH variations, and finally concluded that the adsorption of Sc^{3+} onto 0.075-AA-0.072@MIL-101 was mediated by cation exchange and coordination reactions. Similarly, Kavun et al. [32] deduced that the adsorption of Er^{3+} ions onto MIL-101-H50 was mediated by coordinative complexes. Using a similar analytical approach, Zhang et al. [65] found that the adsorption of Nd^{3+} by agaric-like U6N@ZIF-8-20 was controlled by cation exchange and chelation reaction involving $-NH_2$ with REEs. It was generally observed that researchers reported electrostatic interactions and chemical sorption as the primary attachment mechanisms involved in the adsorption of REE by MOFs.

7. Regeneration of metal–organic framework

The ability to recover adsorbed ions and regenerate the adsorbent is decisive for the economic and environmental sustainability of an adsorption process [80]. Additionally, regeneration studies can provide valuable insights into adsorption mechanisms [27]. According to Omorogie et al. [81], adsorbent regeneration methods are typically classified into thermal techniques (e.g., inert gas, steam, and microwave) and nonthermal techniques (e.g., solvent extraction, ultrasound, and complexation).

Nonthermal methods, particularly those utilizing solvents, have been shown to alter the interactions between the sorbate and sorbent, such as electrostatic forces, hydrophobic effects, π–π interactions, and hydrogen bonding, thereby enhancing the desorption process [82]. An ideal eluent must be cost-effective, environmentally friendly, highly efficient, and nondestructive to the adsorbent's properties [76].

Zhou et al. [62] conducted desorption studies using methanol as an eluent, successfully releasing 75% of adsorbed Ce^{3+} ions after the first cycle. However, a significant loss in efficiency was observed after three cycles, with adsorption efficiency dropping by 90% (**Table 3**). By contrast, Lee et al. [70] used 0.1 M HCl to desorb Gd^{3+} ions from MIL-101-PMIDA. After five adsorption–desorption cycles, the adsorbent retained most of its functional groups and structural stability, with less than a 10% loss in efficiency (**Table 3**).

Lou et al. [66] reported on the desorption of Sc^{3+} from 0.075-AA-0.072@MIL-101 using various eluents, including acetic acid, HCl, HNO_3, and H_2SO_4. Elution with 0.3 M HCl at 30°C for 3 h showed excellent performance in releasing Sc^{3+}. After five adsorption–desorption cycles, more than 80% of the adsorption potential remained intact. X-ray diffraction (XRD) analysis confirmed the structural integrity of 0.075-AA-0.072@MIL-101, demonstrating the adsorbent's excellent reusability.

Among the reviewed literature, the optimal eluents were HCl, HNO_3, and acetonitrile, with an average of five attainable adsorption–desorption cycles. While significant loss in adsorption efficiency was reported after five cycles, most MOFs performed exceptionally well within the first three cycles, with minimal losses observed. Zhang et

al. [60] successfully desorbed Y^{3+} from linker-defective MIL-101(Cr)-D MOF using 0.5 M EDTA. Their study uniquely investigated the structural changes of the MOF following multiple adsorption–desorption cycles. XRD analysis revealed that the crystalline structure of the adsorbent underwent complete disintegration after 12 successive cycles, highlighting the limitations of its structural stability under prolonged use.

Table 3 • Metal–organic framework regeneration following rare earth element adsorption

Adsorbent	Adsorbate	Eluent	Adsorption–desorption cycles	Loss in adsorption efficiency	Ref.
MIL-101-PMIDA	Gd^{3+}	0.1 M HCl	5	≈10%	[70]
LaBDC@50%PEI	Gd^{3+}	0.1 M HCl	5	≈50%	[71]
0.075-AA-0.072@MIL-101	Sc^{3+}	0.3 M HCl	5	≈20%	[66]
MIL-101-H50	Er^{3+}	1.0 M HNO_3	3	≈55%	[32]
U6N@ZIF-8-20	Nd^{3+}	Acetonitrile	5	0% for the first 3 cycles; ≈38% after 5 cycles	[65]
HKUST-1 MOF	Ce^{3+}	Methanol	3	≈90%	[62]
P-MNPC@SiO_2	Ce^{3+}	EDTA	5	19%	[67]
MIL-101(Cr)-SMA-ED-PMG	Eu^{3+}	0.3 M HCl or 0.3 M HNO_3	5	13%	[59]
UiO-66-COOH-DETA	Tb^{3+}	0.2 M HCl	3	9%	[83]
MIL-101(Cr)-NH-DTPA	La^{3+}	0.1 M HCl	5	7%	[84]
PMIDA@FeBTC	La^{3+}	0.1 M HNO_3	5	≈15%	[68]
MIL-101(Cr)-D	Yb^{3+}	0.05 M EDTA	12	50%	[60]

Many MOFs lack chemical stability, especially in harsh environments, such as acidic or aqueous conditions, which limits their large-scale application. However, ZIF-8 (a Zn-based imidazolate framework) and UiO-66 (a Zr-based MOF) stand out for their exceptional chemical and thermal stability. Recently published studies have demonstrated promising alternatives, such as MIL-101(Cr)-SMA-ED-PMG [59], MIL-101-PMIDA [70], and MIL-101(Cr)-D [60], which maintained structural integrity and exhibited minimal efficiency loss even after multiple desorption cycles in acidic solutions.

These findings bode well for the continued development of MOFs in REE recovery. While these studies primarily focused on adsorbent stability through multiple adsorption–desorption cycles, research on the long-term recovery and reuse of REEs remains limited. Additionally, none of the reviewed studies addressed the safe disposal of spent adsorbents. Tackling these challenges will be crucial in enhancing the viability of MOFs for REE adsorption systems.

8. The application of metal–organic frameworks for rare earth element adsorption in real-world scenarios

As MOFs have only recently been explored for REE adsorption and recovery, research has primarily concentrated on batch-scale experiments using single-ion synthetic solutions. However, several efforts have been made to better simulate real-world conditions. De Decker et al. [58] investigated the adsorption of Eu^{3+} in the presence of competing REE ions, specifically Y^{3+} and Zn^{2+}, to assess selectivity under mixed REE–ion conditions. Liang and Zeng [58] extended this approach by studying Eu^{3+} removal from simulated zinc ore wastewater, thereby incorporating a more complex matrix. Gao et al. [84] further advanced this research by simulating ammonium-rich wastewater and evaluating the removal efficiency of heavy, medium, and light REEs, viz. Er^{3+}, Eu^{3+}, and La^{3+}, respectively. Their study aimed to replicate effluent conditions characteristic of rare earth metallurgical processes, where ammonium salts are extensively used for rare earth oxide precipitation, leading to high concentrations of NH_4^+-N in wastewater. The adsorbent MIL-101(Cr)-NH-DTPA achieved a 70% REE recovery rate, highlighting its potential for practical application.

In contrast to synthetic wastewater studies, Zhang et al. [85] conducted a notable investigation using real REE mining wastewater. They examined the adsorption performance of a ZIF-8@ALG composite hydrogel for recovering REEs from wastewater containing 13 REEs, including La, cerium (Ce), praseodymium (Pr), neodymium (Nd), europium (Eu), terbium (Tb), dysprosium (Dy), holmium (Ho), erbium (Er), ytterbium (Yb), Lu, and Y. The study reported no significant reduction in adsorption efficiency for most REEs, except for Y, even after four adsorption–desorption cycles. Additionally, the adsorbent maintained its structural integrity, demonstrating excellent stability and reusability.

Progress toward real-world application has been achieved through investigations involving competing ion effects, synthetic wastewater systems, and real mining wastewater. However, to facilitate the transition from laboratory research to industrial application, further studies utilizing laboratory-scale column experiments are necessary. Such investigations will provide a more accurate assessment of MOF performance under continuous-flow conditions, bringing REE adsorption technology closer to large-scale deployment.

A significant challenge in advancing MOF technology stems from their synthesis as nanoparticles. While these nanoparticles offer

advantages such as increased surface area and enhanced adsorption capacity, they present practical limitations in industrial applications. Nanoparticles can be difficult to handle and challenging to recover after use. Fine powders are prone to aggregation and can lead to pressure drops in packed columns, making them unsuitable for continuous-flow systems. In the field of adsorption, researchers have had some success in addressing these MOF challenges through techniques such as granulation [86], pelletization [87], microspheres [88], beads [85], and MOF-based composites [59]. Other approaches that have been gaining momentum include the development of MOF monoliths [89] and gels [90], which effectively tackle the scalability and durability challenges associated with nanosized MOFs. These advancements not only enhance mechanical stability and improve handling but also enable the integration of MOFs into column-based adsorption systems, making them more viable for industrial applications.

Another significant barrier to the widespread application of MOF-based adsorption for REE recovery is the lack of comprehensive cost–benefit analyses encompassing the synthesis, reuse, recovery, and disposal of spent adsorbents. In a promising study, Fonseka et al. [91] conducted a cost–benefit analysis for amine-grafted SBA-15 (SBA-15-NH-PMIDA) as an adsorbent for Eu^{3+} removal from acid mine drainage wastewater. Their findings indicated that the adsorbent could recover 193.2 g of $EuCl_3$ per 1,000 m^3 of treated wastewater. Additionally, the estimated cost of treatment was 3.32 A$/$m^3$, while the potential revenue from the recovered REE was calculated at 13.89 A$/$m^3$. These results underscore the economic viability of MOF-based adsorption systems for REE removal and recovery, highlighting their potential for practical implementation.

9. Future prospects and current gaps

The adsorption of REEs using MOFs presents several advantages, including potentially low capital and operational costs, no sludge production, and the possibility of adsorbent regeneration. Most reported studies focus on laboratory-scale batch investigations using single contaminants in synthetic solutions. Despite the optimization knowledge gathered so far, several areas still require deeper investigation to facilitate the transition to full-scale application. At the laboratory batch scale, more extensive investigations into various operational parameters such as agitation, initial REE concentrations, and MOF dosages are crucial for the efficient design of full-scale batch adsorption systems. Other key areas of focus should include minimizing contact time and applying real wastewater conditions.

An important aspect that warrants further investigation is the potential change in the oxidation state of REE cations during adsorption by MOFs. Occasionally, adsorption may not only involve physical or chemical interactions but could also be accompanied by redox transformations. However, this phenomenon has not been widely reported in the literature reviewed for this study. Future research should explore whether specific MOF structures or functional groups facilitate oxidation or reduction of REEs, as well as the implications of such changes on adsorption efficiency, selectivity, and material stability. Understanding this aspect could provide deeper insights into the adsorption mechanisms and help optimize MOF design for REE recovery.

Additionally, very few studies have explored the application of MOFs in fixed-bed column studies, which are pertinent for understanding the impact of fine MOFs on pressure drop, channeling, and scalability. While desorption studies of REEs from MOFs are well documented, systematic evaluations of REE recovery remain limited. Future research should focus on categorizing recovery methods based on MOF structure, REE type, and experimental conditions. Establishing standardized protocols and optimizing recovery techniques will be essential for advancing MOF-based REE recovery toward industrial applications.

Currently, adsorption research has thoroughly investigated only a fraction of the 17 known REEs. To ensure the broad acceptance and applicability of MOF technology, the scope of REE types studied needs to be expanded. Future research should also focus on the environmental impact of spent MOFs, including their stability, potential leaching, and safe disposal or regeneration strategies. Additionally, comprehensive economic analyses are needed to assess the cost-effectiveness of MOF-based REE recovery, considering synthesis, reuse, and scalability. Evaluating REE recovery methods under real-world conditions will be essential to optimize efficiency and support the transition of MOF technology from laboratory studies to industrial applications.

10. Conclusions

The research conducted thus far on the adsorption of REEs by MOFs has significantly advanced our understanding and laid a solid foundation for broader applications. Functionalization and combination of MOFs have proven effective in enhancing adsorbent capacity, stability, adsorption rate, and reusability. While the average time to reach equilibrium was approximately 4.5 h, some adsorbents achieved equilibrium in under 30 min. In most instances, isothermal and kinetic data followed the Langmuir and pseudo-second-order models. Compared to other adsorbents, MOFs demonstrated favorable adsorption capacities for REEs. Notably, the 3D-agaric-like core–shell U6N@ZIF-8-20 MOF, MOF-bonded silica amine and polymer, and phosphonic acid–functionalized ZIF-67@SiO_2 exhibited adsorption capacities of 341.0, 426.0, and 342.5 mg/g for Er^{3+}, Y^{3+}, and Ce^{3+}, respectively.

Only a fraction of the reviewed studies explored thermodynamic analysis. Among those, the reactions were generally spontaneous and varied between endothermic and exothermic. The primary reported mechanisms for REE attachment were electrostatic attraction and chemical sorption. The selectivity of MOFs for target REEs was extensively studied, with mono- and divalent competing ions having negligible effects, while trivalent ions were only slightly competitive. The reusability of MOFs was also well investigated, identifying efficient eluents such as HCl, HNO_3, and acetonitrile and demonstrating that some MOFs could achieve five adsorption–desorption cycles with negligible decreases in adsorption efficiency.

Most studies focused on single-contaminant systems at the laboratory batch scale. To advance this technology, future research should emphasize reducing equilibrium time, exploring a broader range of REEs, conducting fixed-bed column studies, performing MOF–REE cost analysis, evaluating real-world wastewater, and investigating the safe disposal of spent MOFs.

Funding

The author declares no financial support for the research, authorship, or publication of this article.

Author contributions

The author confirms sole responsibility for this work. The author approves of this work and takes responsibility for its integrity.

Conflict of interest

The author declares no conflict of interest.

Data availability statement

Data supporting these findings are available within the article, at https://doi.org/10.20935/AcadEnvSci7629, or upon request.

Institutional review board statement

Not applicable.

Informed consent statement

Not applicable.

Additional information

Received: 2024-07-25

Accepted: 2025-03-19

Published: 2025-04-04

Academia Environmental Sciences and Sustainability papers should be cited as *Academia Environmental Sciences and Sustainability 2025*, ISSN 2997-6006, https://doi.org/10.20935/AcadEnvSci7629. The journal's official abbreviation is *Acad. Env. Sci. Sust.*

Publisher's note

Copyright

References

1. Feng X, Onel O, Council-Troche M, Noble A, Yoon R-H, Morris JR. A study of rare earth ion-adsorption clays: the speciation of rare earth elements on kaolinite at basic pH. Appl Clay Sci. 2021;201:105920. doi: 10.1016/j.clay.2020.105920
2. Unsworth CE, Kuo CC, Kuzmin A, Khalid S, Saha D. Adsorption of rare earth elements onto DNA-functionalized mesoporous carbon. ACS Appl Mater Interfaces. 2020;12:43180–90. doi: 10.1021/acsami.0c09393
3. Massari S, Ruberti M. Rare earth elements as critical raw materials: focus on international markets and future strategies. Resour Policy. 2013;38:36–43. doi: 10.1016/j.resourpol.2012.07.001
4. Singh Y. Indian rare-earth deposits: related industry, balance problem and atmnirbhar Bharat. Geological and geo-environmental processes on earth. Singapore: Springer Singapore; 2021. p. 91–117.
5. Callura JC, Perkins KM, Noack CW, Washburn NR, Dzombak DA, Karamalidis AK. Selective adsorption of rare earth elements onto functionalized silica particles. Green Chem. 2018;20:1515–26. doi: 10.1039/c8gc00051d
6. Weng Z, Haque N, Mudd GM, Jowitt SM. Assessing the energy requirements and global warming potential of the production of rare earth elements. J Clean Prod. 2016;139:1282–97. doi: 10.1016/j.jclepro.2016.08.132
7. Zaimes GG, Hubler BJ, Wang S, Khanna V. Environmental life cycle perspective on rare earth oxide production. ACS Sustain Chem Eng. 2015;3:237–44. doi: 10.1021/sc500573b
8. Zhang S, Kano N, Mishima K, Okawa H. Adsorption and desorption mechanisms of rare earth elements (REEs) by layered double hydroxide (LDH) modified with chelating agents. Appl Sci. 2019;9:4805. doi: 10.3390/app9224805
9. Xu X, Zou J, Zhao X-R, Jiang X-Y, Jiao F-P, Yu J-G, et al. Facile assembly of three-dimensional cylindrical egg white embedded graphene oxide composite with good reusability for aqueous adsorption of rare earth elements. Colloids Surf A Physicochem Eng Asp. 2019;570:127–40. doi: 10.1016/j.colsurfa.2019.03.022
10. Wang W, Yang Y, Wang D, Huang L. Toxic effects of rare earth elements on human health: a review. Toxics. 2024;12:1–13. doi: 10.3390/toxics12050317
11. Cheng J, Cheng Z, Hu R, Cui Y, Cai J, Li N, et al. Immune dysfunction and liver damage of mice following exposure to lanthanoids: immune dysfunction and liver damage caused by lanthanoids. Environ Toxicol. 2014;29:64–73. doi: 10.1002/tox.20773
12. Liu H, Yuan L, Yang X, Wang K. La^{3+}, Gd^{3+} and Yb^{3+} induced changes in mitochondrial structure, membrane permeability, cytochrome c release and intracellular ROS level. Chem Biol Interact. 2003;146:27–37. doi: 10.1016/s0009-2797(03)00072-3
13. Brouziotis AA, Giarra A, Libralato G, Pagano G, Guida M, Trifuoggi M. Toxicity of rare earth elements: an overview on

human health impact. Front Environ Sci. 2022;10:1–14. doi: 10.3389/fenvs.2022.948041

14. Smith YR, Bhattacharyya D, Willhard T, Misra M. Adsorption of aqueous rare earth elements using carbon black derived from recycled tires. Chem Eng J. 2016;296:102–11. doi: 10.1016/j.cej.2016.03.082
15. Van Nguyen N, Iizuka A, Shibata E, Nakamura T. Study of adsorption behavior of a new synthesized resin containing glycol amic acid group for separation of scandium from aqueous solutions. Hydrometallurgy. 2016;165:51–6. doi: 10.1016/j.hydromet.2015.11.016
16. Rajaniemi K, Tuomikoski S, Lassi U. Electrocoagulation sludge valorization—A review. Resources. 2021;10:127. doi: 10.3390/resources10120127
17. Pereao O, Bode-Aluko C, Fatoba O, Laatikaine K, Petrik L. Rare earth elements removal techniques from water/wastewater: a review. Desalin Water Treat. 2018;130:71–86. doi: 10.5004/dwt.2018.22844
18. Stratiotou Efstratiadis V, Michailidis N. Sustainable recovery, recycle of critical metals and rare earth elements from waste electric and electronic equipment (circuits, solar, wind) and their reusability in additive manufacturing applications: a review. Metals. 2022;12:794. doi: 10.3390/met12050794
19. Castro L, Blázquez ML, González F, Muñoz JÁ. Biohydrometallurgy for rare earth elements recovery from industrial wastes. Molecules. 2021;26:6200. doi: 10.3390/molecules26206200
20. Dushyantha N, Ilankoon ISK, Ratnayake NP, Premasiri HMR, Dharmaratne PGR, Abeysinghe AMKB, et al. Recovery potential of rare earth elements (REEs) from the gem mining waste of Sri Lanka: a case study for mine waste management. Minerals. 2022;12:1–13. doi: 10.3390/min12111411
21. Rybak A, Rybak A, Joostberens J. The role of clean coal technologies in the development of renewable energy sources. Energies. 2024;17:2892. doi: 10.3390/en17122892
22. Liu P, Zhao S, Xie N, Yang L, Wang Q, Wen Y, et al. Green approach for rare earth element (REE) recovery from coal fly ash. Environ Sci Technol. 2023;57:5414–23. doi: 10.1021/acs.est.2c09273
23. Kulczycka J, Kowalski Z, Smol M, Wirth H. Evaluation of the recovery of rare earth elements (REE) from phosphogypsum waste-case study of the WIZÓW chemical plant (Poland). J Clean Prod. 2016;113:345–54. doi: 10.1016/j.jclepro.2015.11.039
24. Salman AD, Juzsakova T, Rédey Á, Le P-C, Nguyen XC, Domokos E, et al. Enhancing the recovery of rare earth elements from red mud. Chem Eng Technol. 2021;44:1768–74. doi: 10.1002/ceat.202100223
25. Echeverry-Vargas L, Ocampo-Carmona LM. Recovery of rare earth elements from mining tailings: a case study for generating wealth from waste. Minerals. 2022;12:948. doi: 10.3390/min12080948
26. Hermassi M, Granados M, Valderrama C, Ayora C, Cortina JL. Recovery of rare earth elements from acidic mine waters: an unknown secondary resource. Sci Total Environ. 2022;810:152258. doi: 10.1016/j.scitotenv.2021.152258
27. Sutherland C, Chittoo BS, Venkobachar C. Application of ANN predictive model for the design of batch adsorbers - equilibrium simulation of Cr(VI) adsorption onto activated carbon. Open Civ Eng J. 2019;13:69–81. doi: 10.2174/1874149501913010069
28. Ashour RM, Abdelhamid HN, Abdel-Magied AF, Abdel-Khalek AA, Ali MM, Uheida A, et al. Rare earth ions adsorption onto graphene oxide nanosheets. Solvent Extr Ion Exch. 2017;35:91–103. doi: 10.1080/07366299.2017.1287509
29. Pinheiro RF, Grimm A, da Boit Martinello K, Khan MR, Ahmad N, Silva LFO, et al. Vine pruning waste-based activated carbon for cerium and lanthanum adsorption from water and real leachate. J Rare Earths. 2024;42:1960–8. doi: 10.1016/j.jre.2023.10.020
30. Liu X, Zhou F, Chi R, Feng J, Ding Y, Liu Q. Preparation of modified montmorillonite and its application to rare earth adsorption. Minerals. 2019;9:747. doi: 10.3390/min9120747
31. Gallardo K, Castillo R, Mancilla N, Remonsellez F. Biosorption of rare-earth elements from aqueous solutions using walnut shell. Front Chem Eng. 2020;2;1–10. doi: 10.3389/fceng.2020.00004
32. Kavun V, van der Veen MA, Repo E. Selective recovery and separation of rare earth elements by organophosphorus modified MIL-101(Cr). Microporous Mesoporous Mater. 2021;312:110747. doi: 10.1016/j.micromeso.2020.110747
33. Ighalo JO, Omoarukhe FO, Ojukwu VE, Iwuozor KO, Igwegbe CA. Cost of adsorbent preparation and usage in wastewater treatment: a review. Clean Chem Eng. 2022;3:100042. doi: 10.1016/j.clce.2022.100042
34. Thallapally PK, Grate JW, Motkuri RK. Facile xenon capture and release at room temperature using a metal-organic framework: a comparison with activated charcoal. Chem Commun. 2012;48:347–9. doi: 10.1039/c1cc14685h
35. Sutherland C. Exploring the state-of-the-art in metal-organic frameworks for antibiotic adsorption: a review of performance, mechanisms, and regeneration. Environ Toxicol Chem. 2025;44;880–94. doi: 10.1093/etojnl/vgaf009
36. Tambat SN, Sane PK, Suresh S, Varadan ON, Pandit AB, Sontakke SM. Hydrothermal synthesis of NH2 -UiO-66 and its application for adsorptive removal of dye. Adv Powder Technol. 2018;29;2626–32. doi: 10.1016/j.apt.2018.07.010
37. Wu Z, Chen Z, Chen J, Ning X, Chen P, Jiang H, et al. Enhanced adsorption and synergistic photocatalytic degradation of tetracycline by MOF-801/GO composites via solvothermal synthesis. Environ Sci Nano. 2022;9:4609–18. doi: 10.1039/d2en00809b
38. Yu K, Lee Y-R, Seo JY, Baek K-Y, Chung Y-M, Ahn W-S. Sonochemical synthesis of Zr-based porphyrinic MOF-525 and MOF-545: enhancement in catalytic and adsorption properties. Microporous Mesoporous Mater. 2021;316:110985. doi: 10.1016/j.micromeso.2021.110985
39. Gul Zaman H, Baloo L, Kutty SR, Aziz K, Altaf M, Ashraf A, et al. Insight into microwave-assisted synthesis of the chitosan-MOF composite: Pb (II) adsorption. Environ Sci Pollut Res. 2023;30:6216–33. doi: 10.1007/s11356-022-22438-6

40. de Lima Neto OJ, Frós AC de O, Barros BS, de Farias Monteiro AF, Kulesza J. Rapid and efficient electrochemical synthesis of a zinc-based nano-MOF for Ibuprofen adsorption. New J Chem. 2019;43:5518–24. doi: 10.1039/c8nj06420b

41. Lv D, Chen Y, Li Y, Shi R, Wu H, Sun X, et al. Efficient mechanochemical synthesis of MOF-5 for linear alkanes adsorption. J Chem Eng Data. 2017;62:2030–6. doi: 10.1021/acs.jced.7b00049

42. Zhao X, Zheng M, Gao X, Zhang J, Wang E, Gao Z. The application of MOFs-based materials for antibacterials adsorption. Coord Chem Rev. 2021;440:213970. doi: 10.1016/j.ccr.2021.213970

43. Huang L, Shen R, Shuai Q. Adsorptive removal of pharmaceuticals from water using metal-organic frameworks: a review. J Environ Manage. 2021;277:111389. doi: 10.1016/j.jenvman.2020.111389

44. Essalmi S, Lotfi S, BaQais A, Saadi M, Arab M, Ait Ahsaine H. Design and application of metal organic frameworks for heavy metals adsorption in water: a review. RSC Adv. 2024;14:9365–90. doi: 10.1039/d3ra08815d

45. Yaghi OM, Li G, Li H. Selective binding and removal of guests in a microporous metal–organic framework. Nature. 1995;378:703–6. doi: 10.1038/378703a0

46. Alezi D, Belmabkhout Y, Suyetin M, Bhatt PM, Weseliński ŁJ, Solovyeva V, et al. MOF crystal chemistry paving the way to gas storage needs: aluminum-based soc-MOF for CH4, O2, and CO2 storage. J Am Chem Soc. 2015;137:13308–18. doi: 10.1021/jacs.5b07053

47. Della Rocca J, Liu D, Lin W. Nanoscale metal-organic frameworks for biomedical imaging and drug delivery. Acc Chem Res. 2011;44:957–68. doi: 10.1021/ar200028a

48. García-García P, Müller M, Corma A. MOF catalysis in relation to their homogeneous counterparts and conventional solid catalysts. Chem Sci. 2014;5:2979. doi: 10.1039/c4sc00265b

49. Lim D-W, Ha J, Oruganti Y, Moon HR. Hydrogen separation and purification with MOF-based materials. Mater Chem Front. 2021;5:4022–41. doi: 10.1039/d1qm00234a

50. Shen Y, Tissot A, Serre C. Recent progress on MOF-based optical sensors for VOC sensing. Chem Sci. 2022;13:13978–4007. doi: 10.1039/d2sc04314a

51. Cai YY, Yang Q, Zhu ZY, Sun QH, Zhu AM, Zhang QG, et al. Achieving efficient proton conduction in a MOF-based proton exchange membrane through an encapsulation strategy. J Memb Sci. 2019;590:117277. doi: 10.1016/j.memsci.2019.117277

52. Shah SSA, Najam T, Cheng D, Hafeez A, Lu Y, Waseem A. Nano-metal organic frame work an excellent tool for biomedical imaging. Curr Med Imaging. 2018;14:669–74. doi: 10.2174/1573405613666170919151454

53. Alrefaee SH, Aljohani M, Alkhamis K, Shaaban F, El-Desouky MG, El-Bindary AA, et al. Adsorption and effective removal of organophosphorus pesticides from aqueous solution via novel metal-organic framework: adsorption isotherms, kinetics, and optimization via Box-Behnken design. J Mol Liq. 2023;384:122206. doi: 10.1016/j.molliq.2023.122206

54. Fan Y, Lu T, Wang X, Lu G, Tong K, Wang Q, et al. Fabrication of dual-functional Zr-based MOF incorporating amino and sulfoxide derivatives for simultaneous removal and detection of tetracycline antibiotics. Sep Purif Technol. 2024;339:126676. doi: 10.1016/j.seppur.2024.126676

55. Elsherbiny AS, Rady A, Abdelhameed RM, Gemeay AH. Efficiency and selectivity of cost-effective Zn-MOF for dye removal, kinetic and thermodynamic approach. Environ Sci Pollut Res Int. 2023;30:106860–75. doi: 10.1007/s11356-023-25919-4

56. Bhadane P, Mahato P, Menon D, Satpathy BK, Wu L, Chakraborty S, et al. Hydrolytically stable nanosheets of Cu–imidazolate MOF for selective trapping and simultaneous removal of multiple heavy metal ions. Environ Sci Nano. 2024;11:2385–96. doi: 10.1039/d3en00754e

57. Villalgordo-Hernández D, Antonio Diaz-Perez M, Balloi V, Anabel Lara-Angulo M, Narciso J, Carlos Serrano-Ruiz J, et al. Post-synthetic ligand exchange as a route to improve the affinity of ZIF-67 towards CO_2. Chem Eng J. 2023;476:146846. doi: 10.1016/j.cej.2023.146846

58. de Decker J, de Clercq J, Vermeir P, van der Voort P. Functionalized metal-organic-framework CMPO@MIL-101(Cr) as a stable and selective rare earth adsorbent. J Mater Sci. 2016;51:5019–26. doi: 10.1007/s10853-016-9807-9

59. Liang X, Zeng Q. Copolymers-functionalized metal-organic framework composite for efficient adsorption of rare-earth elements. Microporous Mesoporous Mater. 2024;366:112960. doi: 10.1016/j.micromeso.2023.112960

60. Zhang Y, Sun C, Ji Y, Bi K, Tian H, Wang B. Engineering linker-defects of MIL-101 series metal organic frameworks for boosted Yb(III) adsorption. Sep Purif Technol. 2024;330:125293. doi: 10.1016/j.seppur.2023.125293

61. Sun C, Ji Y, Bi K, Tian H, Wang C, Deng F, et al. Tuning oxygen vacancy and missing linkers of defective MOF-808 for advanced adsorption of Yb(III) from aqueous solution. Sep Purif Technol. 2024;347:127585. doi: 10.1016/j.seppur.2024.127585

62. Zhao L, Azhar MR, Li X, Duan X, Sun H, Wang S, et al. Adsorption of cerium (III) by HKUST-1 metal-organic framework from aqueous solution. J Colloid Interface Sci. 2019;542:421–8. doi: 10.1016/j.jcis.2019.01.117

63. Ammari Allahyari S, Saberi R, Sepanloo K, Lashkari A. Adsorptive separation of La(III) from aqueous solution via the synthesized [Zn(bim)2(bdc)] metal-organic framework. J Rare Earths. 2021;39:742–8. doi: 10.1016/j.jre.2020.07.027

64. Komnitsas K, Zaharaki D, Bartzas G, Alevizos G. Adsorption of scandium and neodymium on biochar derived after low-temperature pyrolysis of sawdust. Minerals. 2017;7:200. doi: 10.3390/min7100200

65. Zhang M, Yang K, Cui J, Yu H, Wang Y, Shan W, et al. 3D-agaric like core-shell architecture UiO-66-NH2@ZIF-8 with robust stability for highly efficient REEs recovery. Chem Eng J. 2020;386:124023. doi: 10.1016/j.cej.2020.124023

66. Lou Z, Xiao X, Huang M, Wang Y, Xing Z, Xiong Y. Acrylic acid-functionalized metal–organic frameworks for Sc(III)

selective adsorption. ACS Appl Mater Interfaces. 2019; 11:11772–81. doi: 10.1021/acsami.9b00476

67. Xu D, Qin Y, Cao X, Huang Y, Wang J, Liu X, et al. Study on the adsorption of Ce(III) on phosphonic acid functionalized ZIF-67@SiO2 magnetic porous carbon materials. Colloids Surf A Physicochem Eng Asp. 2024;696:134306. doi: 10.1016/j.colsurfa.2024.134306
68. Sinha S, De S, Mishra D, Shekhar S, Agarwal A, Sahu KK. Phosphonomethyl iminodiacetic acid functionalized metal organic framework supported PAN composite beads for selective removal of La(III) from wastewater: adsorptive performance and column separation studies. J Hazard Mater. 2022;425:127802. doi: 10.1016/j.jhazmat.2021.127802
69. Mahmoud ME, Mohamed AK, Amira MF, Seleim SM. Novel nanostructured metal–organic framework-bonded silica Amine and polymer: facile synthesis, kinetics, isotherms, and thermodynamics evaluation for adsorption of yttrium(III) ions. J Chem Eng Data. 2019;64:6060–70. doi: 10.1021/acs.jced.9b00918
70. Lee Y-R, Yu K, Ravi S, Ahn W-S. Selective adsorption of rare earth elements over functionalized Cr-MIL-101. ACS Appl Mater Interfaces. 2018;10:23918–27. doi: 10.1021/acsami.8b07130
71. Li W, Huang L, Xiao B, Duan X, Li H, Li L, et al. Efficient and selective recovery of Gd(III) via polyethyleneimine modification of lanthanum-based metal–organic frameworks. J Rare Earths. 2024;42:210–9. doi: 10.1016/j.jre.2022.11.003
72. Wu J, Li Z, Tan H, Du S, Liu T, Yuan Y, et al. Highly selective separation of rare earth elements by Zn-BTC metal–organic framework/nanoporous graphene via in situ green synthesis. Anal Chem. 2021;93:1732–9. doi: 10.1021/acs.analchem.0c04407
73. Iannicelli-Zubiani EM, Gallo Stampino P, Cristiani C, Dotelli G. Enhanced lanthanum adsorption by amine modified activated carbon. Chem Eng J. 2018;341:75–82. doi: 10.1016/j.cej.2018.01.154
74. Hamed MM, Rizk SE, Nayl AA. Adsorption kinetics and modeling of gadolinium and cobalt ions sorption by an ion-exchange resin. Part Sci Technol. 2016;34:716–24. doi: 10.1080/02726351.2015.1112328
75. Delgado-Marín JJ, Izan DP, Molina-Sabio M, Ramos-Fernandez EV, Narciso J. New generation of MOF-monoliths based on metal foams. Molecules. 2022;27:1968. doi: 10.3390/molecules27061968
76. Sutherland C, Chittoo BS, Samlal A. The status of scientific development on the application of biosorption of heavy metals at laboratory and pilot-scale: a review. Desalin Water Treat. 2023;299:13–49. doi: 10.5004/dwt.2023.29699
77. Saha P, Chowdhury S. Insight into adsorption thermodynamics. In: Tadashi M, editor. Thermodynamics. Croatia: InTech; 2011. p. 349–64.
78. Sutherland C. Adsorption of cephalexin: a decade of progress in adsorbent development and mechanistic insights. Desalin Water Treat. 2024;318:100357. doi: 10.1016/j.dwt.2024.100357
79. Sutherland C, Chittoo BS, Venkobachar C. A comparative study of hybrid artificial neural network models for predicting Cr(VI) adsorption onto activated carbon. Desalin Water Treat. 2018; 103:182–98. doi: 10.5004/dwt.2018.21930
80. Kulkarni S, Kaware J. Regeneration and recovery in adsorption-a review. Int J Innov Sci Eng Technol. 2014;1:61–4.
81. Omorogie MO, Babalola JO, Unuabonah EI. Regeneration strategies for spent solid matrices used in adsorption of organic pollutants from surface water: a critical review. Desalin Water Treat. 2016;57:518–44. doi: 10.1080/19443994.2014.967726
82. Dutta T, Kim T, Vellingiri K, Tsang DCW, Shon JR, Kim K-H, et al. Recycling and regeneration of carbonaceous and porous materials through thermal or solvent treatment. Chem Eng J. 2019;364:514–29. doi: 10.1016/j.cej.2019.01.049
83. Sharaf M, Atrees MS, Saleh GM, Mira HI, Tanaka S. Selective extraction of terbium using functionalized metal–organic framework-based solvent-impregnated mixed-matrix membranes. Compounds. 2024;4:679–87. doi: 10.3390/compounds4040041
84. Gao T, Liu Z, Zhang M, Wang Q, Yao F, Zhao F, et al. Selectively recovering rare earth elements with carboxyl immobilized metal-organic framework from ammonium-rich wastewater. Environ Res. 2024;262:119890. doi: 10.1016/j.envres.2024.119890
85. Zhang C, Chen W, Owens G, Chen Z. Recovery of rare earth elements from mine wastewater using alginate microspheres encapsulated with zeolitic imidazolate framework-8. J Hazard Mater. 2024;471:134435. doi: 10.1016/j.jhazmat.2024.134435
86. Tu TN, Shin Y, Khalate SA, Chang K, Kwon HT, Kim J. Meso/macropore emerging from MOF granulation for enhancing performance in the Xe/Kr separation. Sep Puri Technol. 2024;343:127128. doi: 10.1016/j.seppur.2024.127128
87. Tsalaporta E, MacElroy JD. A comparative study of the physical and chemical properties of pelletized HKUST-1, ZIF-8, ZIF-67 and UiO-66 powders. Heliyon. 2020;6:1–9. doi: 10.1016/j.heliyon.2020.e04883
88. Yang M, Bai Q. Flower-like hierarchical Ni-Zn MOF microspheres: efficient adsorbents for dye removal. Colloids Surf A Physicochem Eng Asp. 2019;582:123795. doi: 10.1016/j.colsurfa.2019.123795
89. Figueroa–Quintero L, Ramos–Fernández EV, Narciso J. 3D-printed brass monoliths for ZIF-8 synthesis and CO2 conversion: a novel approach using selective laser melting. J Environ Chem Eng. 2025;13(2):115453. doi: 10.1016/j.jece.2025.115453
90. Zhuang Z, Mai Z, Wang T, Liu D. Strategies for conversion between metal–organic frameworks and gels. Coord Chem Rev. 2020;421:213461. doi: 10.1016/j.ccr.2020.213461
91. Fonseka C, Ryu S, Choo Y, Kandasamy J, Foseid L, Ratnaweera H, et al. Selective recovery of europium from real acid mine drainage using modified Cr-MIL and SBA15 adsorbents. Environ Sci Pollut Res Int. 2024;31:51540–50. doi: 10.1007/s11356-024-34566-2